Published in "Developmental Biology 344(2): 593-602 , 2010"
which should be cited to refer to this work.

The *C. elegans* sex determination protein MOG-3 functions in meiosis and binds to the CSL co-repressor CIR-1

Prasad Kasturi, Simone Zanetti, Myriam Passannante, Zarifja Saudan, Fritz Müller, Alessandro Puoti *

Department of Biology, University of Fribourg, Switzerland

In the germ line of the *Caenorhabditis elegans* hermaphrodite, nuclei either proliferate through mitosis or initiate meiosis, finally differentiating as spermatids or oocytes. The production of oocytes requires repression of the *fem-3* mRNA by cytoplasmic FBF and nuclear MOG proteins. Here we report the identification of the sex determining gene *mog-3* and show that in addition to its role in gamete sex determination, it is necessary for meiosis by acting downstream of GLP-1/Notch. Furthermore, we found that MOG-3 binds both to the nuclear proteins MEP-1 and CIR-1. MEP-1 is necessary for oocyte production and somatic differentiation, while the mammalian CIR-1 homolog counters Notch signaling. We propose that MOG-3, MEP-1 and CIR-1 associate in a nuclear complex which regulates different aspects of germ cell development. While FBF triggers the sperm/oocyte switch by directly repressing the *fem-3* mRNA in the cytoplasm, the MOG proteins play a more indirect role in the nucleus, perhaps by acting as epigenetic regulators or by controlling precise splicing events.

Introduction

The proliferation and specification of germ cells provide an excellent system to investigate genetic interactions and gene regulation which lead to specific cell fates in a developing organism. In the hermaphroditic nematode *Caenorhabditis elegans*, germ cells undergo two crucial cell fate decisions. They first choose between proliferation and differentiation. Then with *C. elegans* hermaphrodites that produce gametes of both sexes, germ cells that are about to undergo meiosis have already been determined for spermatogenesis or oogenesis (for reviews, see Hubbard and Greenstein, 2005; Kimble and Crittenden, 2007). After limited numbers of spermatids have been produced in the L4 larva, adult hermaphrodites switch to oogenesis for the rest of their lives. The switch from spermatogenesis to oogenesis is dependent on the repression of the *fem-3* mRNA (Ahringer et al., 1992). If *fem-3* repression is abrogated, hermaphrodite germ lines are masculinized and produce excess sperm (Barton et al., 1987). *fem-3* is post-transcriptionally regulated through a *cis*-acting element in its 3′ untranslated region (UTR) (Ahringer and Kimble, 1991). The two redundant RNA binding proteins FBF-1 and FBF-2 (*fem-3 b*inding *f*actor) bind directly to this *cis*-acting regulatory element to repress *fem-3* expression. With both *fbf* genes inactivated, hermaphrodites make excess sperm instead of switching to oogenesis (Crittenden et al., 2002; Zhang et al., 1997). The repression by FBF requires NOS-3, but is also controlled through GLD-3 and RNP-8 which compete with each other for binding to GLD-2, the catalytic subunit of a cytoplasmic poly(A) polymerase (Eckmann et al., 2002; Kraemer et al., 1999; Kim et al., 2009). In addition to their roles in the sperm–oocyte switch, FBF and NOS play essential roles in germ line proliferation (Crittenden et al., 2002; Kraemer et al., 1999; Lamont et al., 2004; Subramaniam and Seydoux, 1999). On the other hand, six *mog* genes are also necessary for the switch from spermatogenesis to oogenesis (Graham and Kimble, 1993; Graham et al., 1993). The *mog* genes are required for *fem-3* repression but their molecular action remains enigmatic (Belfiore et al., 2004; Gallegos et al., 1998; Puoti and Kimble, 1999, 2000). One indication, however, is that all MOG proteins cloned to date are related to splicing factors. For example, MOG-1 and MOG-5 are the worm orthologs of spliceosomal proteins Prp16 and Prp22 in *Saccharomyces cerevisiae* (Puoti and Kimble, 1999, 2000). MOG proteins bind to MEP-1, which is necessary for *fem-3* repression (Belfiore et al., 2002). MEP-1 also functions in a chromatin remodeling complex which orchestrates the differentiation between somatic and germline cells (Unhavaithaya et al., 2002). Thus, while the MES proteins establish a stable chromatin state in pluripotent germ cells, MEP-1 remodels chromatin to abolish pluripotency and allow somatic differentiation (Unhavaithaya et al., 2002).

We report the cloning of *mog-3* and its initial characterization. We have found that besides its role in the sperm–oocyte switch, *mog-3* is also required for meiosis. Furthermore, we show that in addition to binding MEP-1, MOG-3 interacts with CIR-1 which functions in several aspects of germline development.

* Corresponding author. Department of Biology, Chemin du Musée 10, 1700 Fribourg, Switzerland. Fax: +41 26 300 9741.
E-mail address: alessandro.puoti@unifr.ch (A. Puoti).

Materials and methods

Strains

All *C. elegans* strains were maintained under standard conditions at 20 °C unless specified otherwise (Brenner, 1974). Strain N2 is wild type. Three recessive temperature sensitive loss-of-function alleles of *mog-3* are available: *q74*, *oz152* and *oz146* (Graham et al., 1993; T. Schedl personal communication). For SNP (single nucleotide polymorphism) analysis, we crossed a *dpy-17(e164)mog-3(oz152)unc-32(e189)* chromosome into polymorphic strain CB4856. Spliced variants and nonsense-mediated decay were tested in *smg-1(r861)I;mog-3(oz152)III* mutants. Alleles *gld-1(q485)I*, *gld-2(q497)I*, *gld-3(q730)II* and *mog-3(oz152)III* were used for the analysis of tumorous phenotypes. The Mog-3 mutant phenotype was visible at restrictive temperature (25 °C). *cir-1(ok1488) I* and *cir-1(tm1601) I* deletion alleles were provided by the CGC and the National BioResource Project. *glp-1* alleles were analyzed in *unc-32(e189)glp-1(oz112)/unc-32(e251)glp-1(q175)III*.

Cloning of mog-3

Recombination frequencies between *mog-3*, *dpy-17* and *unc-32* placed *mog-3* to the right of *dpy-17*. Deletion mapping and analysis of polymorphisms located *mog-3* between two SNPs on cosmids ZK121 (position 7269) and ZC395 (position 27315); (Jakubowski and Kornfeld, 1999). Sequencing of candidate genes from this interval in *mog-3* animals identified mutations in open reading frame F52C9.7.

cDNAs, accession numbers and sequence alignments

Full-length cDNAs were isolated from various oligo dT-primed cDNA libraries. *C. elegans mog-3* is SL1 trans-spliced. *C. remanei mog-3* was recovered from a library that was prepared from strain PB4641. Accession numbers for *mog-3* are DQ641631 (*C. elegans*); DQ641632 (*C. briggsae*) and DQ641633 (*C. remanei*). Accession number for *cir-1* is DQ645890. Sequences were aligned with the DNASTAR® package from Lasergene using the Gonnet protein weight matrix. Gap penalty was set to 10 and gap length penalty was 0.2. Conserved protein domains were found with CDD from NCBI (Marchler-Bauer et al., 2009). An N-terminal domain of CIR homology in the CIR-1 N terminus was found in Pfam 10197 (Fig. S3G). This domain was also present in the N-terminal extension of MOG-3 homologs. Proteins used for MOG-3 alignments were Q6DF5 (*Xenopus*), NP_060218.1 (Human), NP_608705.1 (*Drosophila*), XP_324772.1 (*Neurospora*), NP_080462.1 (Mouse), NP_998627.1 (Zebrafish), CAY82364 is Cwc25 from *S. cerevisiae* and NP_595394.1 is Cwf25 from *S. pombe*.

Northern analysis and RT-PCR

Poly $(A)^+$ RNA or total RNA was extracted and analyzed as described (Puoti and Kimble, 1999). RT-PCR was performed on 1.5 µg of DNAse-treated total RNA from adult wild type, *mog-3* or *smg-1;mog-3* animals (Puoti and Kimble, 1999; Belfiore et al., 2004). Genomic DNA and oligo (dT)-primed single-stranded cDNAs from wild type animals were used as controls. Primer sequences are available on request.

RNA interference

Sense and anti-sense *mog-3* (1–643 nt) or *cir-1* (350–1050 nt) RNAs were generated using T3 and T7 RNA polymerases (Stratagene). RNA interference was performed by injecting dsRNA (1.5 µg/µl for *mog-3* and 0.5 µg/µl for *cir-1*) into young adult worms, by feeding HT115 bacteria expressing *cir-1* dsRNA at 23 °C (Timmons and Fire, 1998) or by soaking L1 larvae (Tabara et al., 1998). For soaking, synchronized L1 larvae were incubated at 20 °C for 68 h in 1 µg/µl of double-stranded *cir-1* RNA or water as a control. Larvae were then transferred to seeded NGM plates and incubated at 25 °C until adulthood, unless specified otherwise.

mog-3 and cir-1 translational fusions

A 5.2 kb *mog-3* genomic fragment, including 2 kb of upstream and 700 bp of downstream sequences was used to generate translational fusion reporters. A NheI site was created 45 nt downstream of the start codon to insert *gfp*. For *cir-1*, this site was 48 nt away from the start codon and 1.9 kb of promoter sequence was used. Both constructs were injected at 10 ng/µl with 40 ng/µl pRF4 marker DNA. Transgenic worms were analyzed by epifluorescence.

Antibodies and immunostaining

Polyclonal antibodies were produced against GST-tagged MOG-3 ($aa_{333-451}$), CIR-1 (aa_{1-355}) or FBF-1 (aa_{1-218}) fusion proteins. For Western blotting, 100 µg of total protein was loaded per lane and analyzed by SDS PAGE. Loading was verified by staining with Ponceau S or by α-Tubulin antibodies (1:2000, Sigma). Blots were incubated in Blotto/Tween with anti-MOG-3 or anti-CIR-1 antibodies (1:500). Secondary HRP IgG conjugates (Sigma) were used at 1:25,000.

For immunostaining, antibodies were diluted 1:50 to 1:200 in PTB (1× PBS, 1% BSA, 1 mM EDTA, 0.5% Triton X-100, and 0.05% NaN_3). Worms were fixed as described (Bettinger et al., 1996) or germ lines were extruded (Francis et al., 1995). Anti-phospho-histone H3 antibody was from Upstate. FITC or Cy-2-conjugated secondary antibodies were diluted 1:1000 (Jackson Immunoresearch). All incubations were performed overnight at 4 °C. Stained worms were mounted with Vectashield containing 2 µg/ml DAPI (4,6-diamino-2-phenylindole) and observed under epifluorescence.

Protein–protein interaction assays and screen

mog-3 cDNA and its derivatives, *lag-1* (nt 600 to stop) and *cir-1* full length cDNAs were introduced into either pBTM116 or pACTII (Bartel and Fields, 1995). A plasmid form of a random-primed cDNA library (λACT-RB2 from R. Barstead) was screened for MOG-3 binding proteins using a MOG-3::LexA fusion construct on minimal medium lacking leucine, tryptophan and histidine, supplemented with 2.5 mM of 3-aminotriazole. Two-hybrid assays were performed in strain L40 (Bartel and Fields, 1995). Positive clones were isolated and tested for β-galactosidase activity (Bai and Elledge, 1997). Positive cDNAs were tested for reciprocal interaction with MOG-3::ACT or with the protein product of an empty bait vector. All constructs were tested for the presence of the fusion protein using either anti-LexA, anti-GAL4 Act or anti-MOG-3 antibodies.

For co-immunoprecipitations, mixed-stage worms were lysed with a Polytron homogenizer in 25 mM HEPES NaOH pH 7.4; 75 mM NaCl; 1 mM DTT; 0.1% TX-100; 1 mM EDTA and protease inhibitors. 10 µl of antiserum was used to capture complexes from 3 mg of protein extract. Protein G beads (rec-Protein G-Sepharose 4B, Zymed Laboratories) were washed with lysis buffer to obtain a 50% slurry and added to the protein precipitate. After incubation overnight at 4 °C, beads were washed several times with lysis buffer supplemented with 50 mM NaCl. Precipitates were analyzed by immunoblotting (1:200 for anti-MEP-1 and 1:900 for anti-CIR-1).

Results

mog-3 is synthetically required for meiosis

At restrictive temperature, *mog*-3 hermaphrodites fail to switch from spermatogenesis to oogenesis and accumulate excess of sperm (Mog, masculinization of the germ line; Graham and Kimble, 1993). *mog-3(q74)/sDf121* heterozygotes are indistinguishable from *mog-3*

homozygotes, indicating that *mog-3* is removed by deficiency *sDf121* (Fig. S1A). Therefore *mog-3(q74)* is either a genetic null allele or a weak allele that is not dose-dependent. At 25 °C *mog-3* hermaphrodites produce on average 800 spermatids per gonad arm (860 ± 118, $n = 10$; Fig. 1A), while *fem-3(gf)* animals make five to ten thousand spermatids (Barton et al., 1987 and Fig. 1B). Therefore *mog-3* is necessary for oogenesis and robust germ line proliferation. In hermaphrodites, meiosis is promoted through two redundant branches that function downstream of GLP/Notch-1. These branches harbor at least *gld-1*, *mog-1*, *-4*, *-5*, *-6* and *nos-3* in the one, and *gld-2* and *gld-3* in the other (Eckmann et al., 2004; Hansen et al., 2004a,b; Belfiore et al., 2004; Kadyk and Kimble, 1998). With two genes from both branches inactivated, meiosis is abrogated and nuclei continue to divide mitotically. Such synthetic tumorous phenotype is due either to defective entry into meiosis or to faulty meiosis progression. While *gld-3* mutant germ lines are feminized (Eckmann et al., 2002; Fig. 1C), *gld-3;mog-3* double mutant germ lines are tumorous (Fig. 1D). In all *gld-3;mog-3* double mutants tested, both the distal and the proximal parts of the gonad are mitotic (Figs. 1E–G). The central region, however, contains nuclei which have initiated meiosis (Fig. 1H). Mitosis marker phospho-histone H3 (PH3) confirmed the presence of mitotic nuclei in both the distal and the proximal portions of the germ line (Fig. 1I). No ectopic PH3 was observed in single *gld-3* and *mog-3* mutants (not shown). Therefore *mog-3* and *gld-3* function synergistically in meiosis progression. The germline tumors in *gld-3;mog-3* hermaphrodites are unlikely to be caused by a synergy between a masculinized germ line and a non functional *gld-3* gene, since *gld-3 (0);fem-3(gf)* germ lines are masculinized and not tumorous (Belfiore et al., 2004). Synthetic tumorous phenotypes were also observed, but to a lesser extent, in *gld-2;mog-3* double mutants (3% Tum, not shown). Similarly, *gld-1(q485)* germ lines are tumorous in that nuclei have a late meiosis onset, but fail to progress through meiotic prophase and instead re-enter mitosis (Fig. 1J; Francis et al., 1995). In contrast, *gld-2 gld-1* germ lines are fully mitotic (Kadyk and Kimble, 1998). We tested a possible synergy between *mog-3* and *gld-1* and found a weak enhancement of the tumorous phenotype: 66% of *gld-1; mog-3* germ lines contained less meiotic nuclei than *gld-1(q485)*, but the remaining 33% were indistinguishable from the single mutant (Figs. 1J,K). *gld-1;mog-3* animals never produced fully mitotic germ lines such as those reported for *gld-2 gld-1* or *glp-1(oz112gf)* hermaphrodites (Berry et al., 1997; Kadyk and Kimble, 1998). Taken together, our results indicate that *mog-3* and *gld-3* act synergistically to promote meiosis progression. This effect was stronger than with *gld-1* and *nos-3*: *mog-3* only weakly enhanced *gld-1* tumors while *nos-3(RNAi)*; *mog-3* germ lines were Mog (data not shown).

mog-3 shares conserved motifs with a putative yeast splicing factor

Genetic mapping located *mog-3* between two SNPs on chromosome *III* (Fig. S1A). Sequencing of candidate genes showed that all

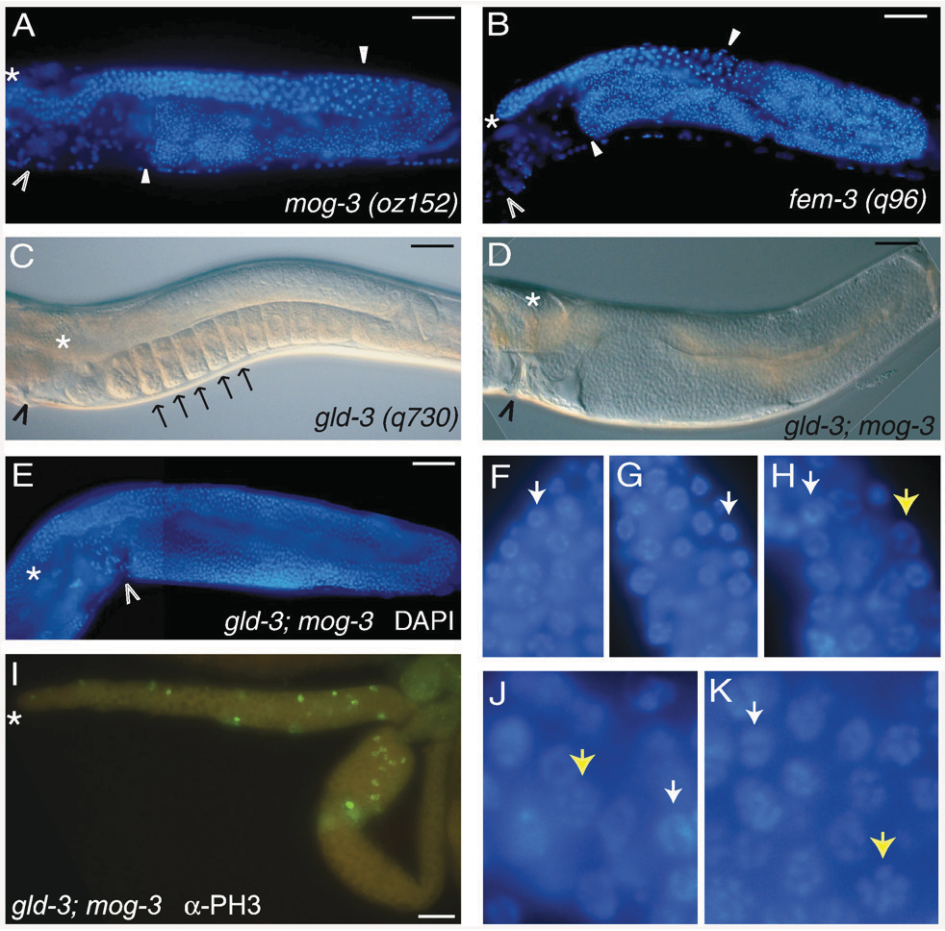

Fig. 1. The Mog-3 mutant phenotype. (A,B) *mog-3*(*oz152*) germ lines are masculinized and contain on average 800 spermatids per gonadal arm. Similarly, gain-of-function alleles of *fem-3*(*q96*) produce only sperm, but in larger amounts (B). The portion of the germ line that is filled with sperm is shown between two white arrowheads. (C) A *gld-3*(*q730*) mutant germ line is feminized. Arrows point towards oocytes. (D–H) *gld-3;mog-3* germ lines are tumorous. Single gonadal arms are shown at low magnification (40× objective; D,E). Details of the proximal (F), distal (G) and central (H) regions of a tumorous *gld-3;mog-3* germ line (100× objective). (I) Anti-phospho-histone H3 staining of a dissected *gld-3;mog-3* gonad. Mitotic nuclei are found throughout the germ line. (J,K) Details of the central region of a *gld-1(q485)* (J) and of a *gld-1(q485);mog-3(oz152)* (K) germ line. Yellow arrows indicate meiotic nuclei. White arrows point towards mitotic nuclei. Open arrowheads point towards the vulva, asterisks indicate the distal end of the germ line. Panels A, B, E–H, J, K: nuclear staining with DAPI. Panels C and D: differential interference contrast (DIC). Scale bar, 10 µm.

available *mog-3* alleles disrupt open reading frame F52C9.7 (Fig. S1A). Furthermore, *mog-3(q74)* was rescued by a wild type copy of F52C9.7. Finally, inactivation of F52C9.7 by RNAi caused a Mog phenotype of weak penetrance (not shown). Therefore, *mog-3* corresponds to gene F52C9.7.

Conceptual translation of the *mog-3* cDNA predicted a 53 kD protein of 451 amino acids that is essentially novel. Nevertheless, MOG-3 contains two motifs in its N terminus that are fully conserved from yeasts to vertebrates (Figs. S1B and S3H). Such motifs are found in Cwf25 from *S. pombe* and Cwc25 from *S. cerevisiae*. Cwf25 is a potential component of the nineteen complex, which activates the spliceosome (NTC; Ohi et al., 2002) and Cwc25 functions in the first catalytic reaction of pre-mRNA splicing (Chiu et al., 2009). Although the overall amino acid identity between MOG-3 and Cwf25 was merely 17%, this homology is interesting in the light of the two conserved motifs that are found in various species (Fig. S3H). In addition MOG-3 contains an arginine and serine-rich RS domain which is found in numerous splicing factors (Fu, 1995). Unlike their orthologs in yeasts, *Drosophila* and vertebrates, MOG-3 homologs from other *Caenorhabditis* species lack an N-terminal extension of 70 amino acids. The significance of the N terminus in non-nematode species will be discussed later (Fig. S3G). The *C. briggsae* and *C. remanei* orthologs share 72% and 75% of overall amino acid identity with *C. elegans* MOG-3, respectively.

A possible role of *mog-3* in splicing was investigated by analyzing *fem-3* and other mRNAs by RT-PCR and Northern blotting. We found that at least general splicing was unaffected in *mog-3* mutants. Results are shown in the supplemental section (Fig. S2).

MOG-3 is mainly expressed in the oocyte lineage

The steady-state levels of the *mog-3* transcript throughout embryonic and larval development indicate that *mog-3* is expressed in embryos and during late larval development, when hermaphrodites switch to oogenesis (Fig. 2A). A *mog-3::gfp* transgene expressed in most tissues of the embryo but also in larvae and adults (Figs. 2B–H). The MOG-3::GFP fusion protein was essentially present in the nucleus, as predicted by two nuclear localization signals (Fig. S1B). The transgene partially rescued the Mog phenotype of *mog-3(oz152)* homozygotes grown at 25 °C since we found 72% of transgenic fertile adults, while in the absence of the transgene, only 15% were fertile. Using antibodies against MOG-3 we found one major 53 kD protein in extracts from wild type and masculinized *fem-3(gf)* animals, but not in *mog-3* mutants (Fig. 2I). MOG-3 was more abundant in wild type than in *fem-3(gf)*

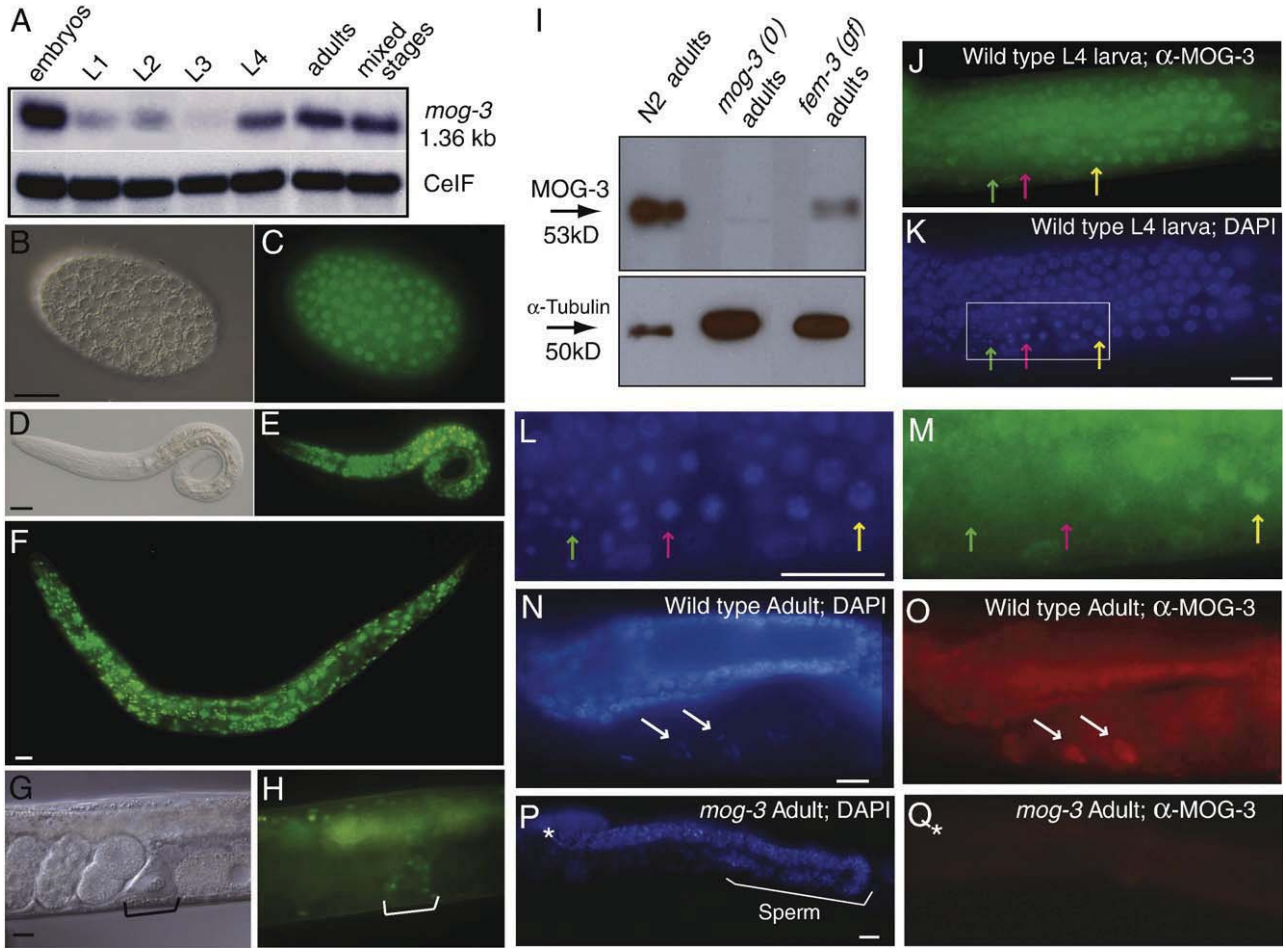

Fig. 2. Expression of *mog-3*. (A) Analysis of the *mog-3* mRNA by Northern blotting. L1 to L4 indicate larval stages. The CelF transcript was used as a loading control. (B–H) Nuclear expression of *mog-3::gfp* in blastomeres at late gastrulation (B,C; 150-cell embryo), in L1 larvae (D,E), young adults (F) and somatic cells of the spermatheca (indicated by a bracket in G,H). B, D and G are DIC images. (I) Western analysis of protein extracts from wild type, masculinized *mog-3(q74 lf)* and *fem-3(q96 gf)* mutants. A 53 kD protein corresponding to the predicted size of MOG-3 was detected in extracts from wild type and *fem-3(gf)* worms, but not in *mog-3(0)* mutants. Anti-α-tubulin antibodies were used as loading control. (J–Q) Immunocytochemistry. Wild type L4, young adult and *mog-3* worms were stained with affinity-purified anti-MOG-3 antibodies. In L4 larvae, MOG-3 was found in almost all nuclei throughout the germ line, including primary spermatocytes (yellow arrow), but not in secondary spermatocytes (pink arrow) and spermatids (green arrow, J–M). Panels L and M are magnifications of the boxed region in J and K. In wild type adults, MOG-3 is also expressed in nuclei of oocytes (N,O). *mog-3* mutants did not stain (P,Q). Nuclei were stained by DAPI (K,L,N,P). Asterisks indicate the distal portion of the germ line. Scale bar, 10 μm.

animals indicating that the protein is expressed in embryos or oocytes, which are absent in the masculinized *fem-3(gf)* mutant. In the germ line, MOG-3 was found in all mitotic and meiotic nuclei, except in secondary spermatocytes and spermatids (Figs. 2J–O). No staining was detected in *mog-3* mutants indicating that the antibody is specific (Figs. 2P,Q). Hence, MOG-3 is a ubiquitous nuclear protein that is mainly present in the oocyte lineage.

MOG-3 binds to MEP-1

Previous studies have shown that the nuclear zinc finger protein MEP-1 binds to MOG proteins (Belfiore et al., 2002, 2004). Here we show that a MOG-3::LexA fusion protein binds to MOG-1, to itself and to MEP-1 (Fig. 3A), but does not interact with MOG-4, MOG-5, MOG-6, FBF-1, GLD-3 and NOS-3 (Fig. 3A). The interaction between MOG-3 and MEP-1 in vivo was confirmed by immunoprecipitation (Fig. 3B).

Deletion derivatives of MOG-3 indicate that the N-terminal portion is necessary and sufficient for binding to MEP-1 (Fig. 3C, rows 1 to 4). However the conserved motifs in the N terminus of MOG-3 are neither sufficient nor necessary for MEP-1 binding (Fig. 3C, rows 4 to 6).

MOG-3 interacts with the CBF/Su(H)/LAG-1 co-repressor CIR-1

We screened a *C. elegans* two-hybrid library for additional MOG-3 binding proteins. Besides more than 20 clones of *mep-1*, we found three cDNAs of a gene which was named *cir-1* (Fig. 4A). CIR-1 is homologous to mammalian CIR, a component of the co-repressor complex, which associates with CBF1 in mammals (Hsieh et al., 1999). Mammalian CIR and *C. elegans* CIR-1 share 35% of overall amino acid identity. Of particular interest is the "N-terminal domain of CIR" (Pfam domain 10197) which is also present in MOG-3 homologs (Figs. S3G,H). Nevertheless this domain is absent from nematode MOG-3, which lacks the N-terminal extension (Fig. S3I). CIR-1 is likely to be the worm ortholog of CIR because amino acids that are necessary for CBF1 binding are conserved in CIR-1 and no closer homolog to CIR was found in *C. elegans*. Furthermore, we show that CIR-1 binds to LAG-1, the worm ortholog of CBF1 (Fig. 4B). CIR-1 also interacts with itself, with MOG-1 and with MEP-1, but neither with FBF and GLD-3, nor with other MOG proteins (Fig. 4B). Using MOG-3 deletion derivatives, we found two distinct domains of MOG-3 that are necessary and sufficient for CIR-1 and MEP-1 binding: amino acids 101 to 185 of MOG-3 bind to CIR-1 and amino acids 1 to 66 interact with MEP-1 (Figs. 3C and 4C). The interaction between MOG-3 and CIR-1 was confirmed by co-immunoprecipitation (Fig. 4D). Similarly, MEP-1 was co-immunoprecipitated by anti-CIR-1 antibodies indicating that MEP-1, MOG-3 and CIR-1 reside in one protein complex (Fig. 4D).

CIR-1 is expressed in meiotic nuclei

Throughout *C. elegans* development, *cir-1* mRNA steady-state levels are similar to those of *mog-3* (Figs. 2A and 5A). We analyzed CIR-1 expression using polyclonal antibodies, as well as a *cir-1::gfp* translational fusion reporter. The reporter expressed in somatic nuclei of the head and the tail, as well as in the developing L4 vulva (Fig. 5B). The *cir-1* expression in the vulva coincides with *mog-3::gfp*, although the expression of the latter was more widespread (not shown). The presence of CIR-1 in the vulva might account for RNAi-induced defects which we observed in the vulva (Figs. 6C,H). Purified anti-CIR-1 antibodies which specifically recognize a 65 kD protein on Western blots were used for immunocytochemistry (Fig. S3F). Similar to MOG-3, CIR-1 is a nuclear protein, which locates to somatic and germ cells (Fig. 5C). In the germ line, CIR-1 was detected in nuclei of the meiotic region, but not in mitotic nuclei of the distal region. The latter express the mitotic marker phospho-histone H3 (Figs. 5D–F).

cir-1 is essential for larval and germ line development

Two deletion alleles of *cir-1* are available (*tm1061* and *ok1488)*. Both mutants cause 90% of larvae to cease development at larval stage one (Fig. S3A). Occasional escapers (10% of mutants from a heterozygous mother raised at 20 °C) develop until larval stage L2. These animals are lethargic and show defects in nucleolar morphology (Figs. 6A,B). The phenotypes observed in L1 and L2 larvae are identical to those of *cir-1(ok1488);mog-3(oz152)* double mutants indicating that loss of *mog-3* does neither enhance nor rescue *cir-1* larval lethality. In order to analyze possible germ line defects due to reduced levels of *cir-1* in adults, we knocked down *cir-1* by RNA interference.

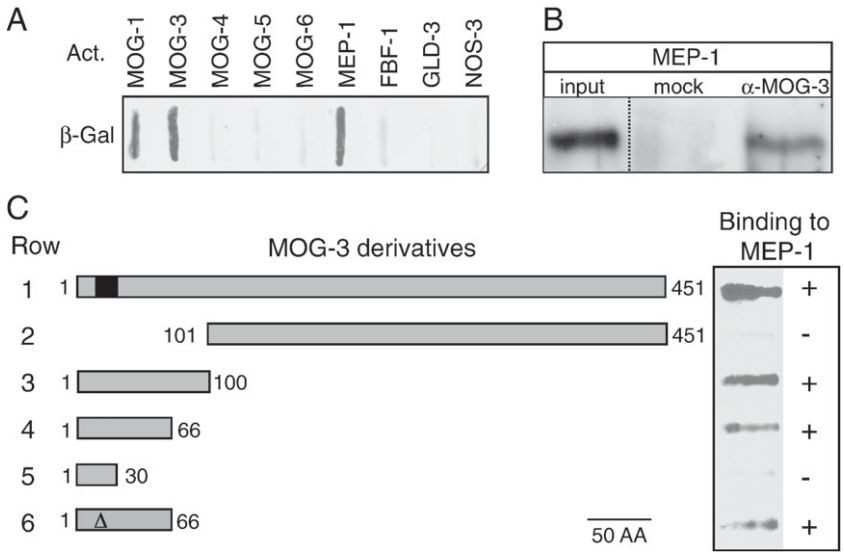

Fig. 3. MOG-3 binds to MEP-1. (A) Protein–protein interactions between MOG-3 and *fem-3* regulators in the yeast two-hybrid system. MOG-3 was fused to the *LexA* DNA binding domain. The other proteins tested were fused to the *GAL4* activation domain (Act.). Blue color indicates positive interaction. (B) Co-immunoprecipitation of wild type worm extracts with either α-MOG-3 or preimmune serum (mock). The blot was probed with anti-MEP-1 antibodies. The dotted line indicates that encompassing lanes have been deleted. MEP-1 migrated at 115 kD. (C) The MOG-3 N terminus is sufficient for MEP-1 binding. Gray boxes indicate MOG-3 protein derivatives. The black box indicates the conserved motifs in MOG-3. Δ, deletion of the conserved motifs.

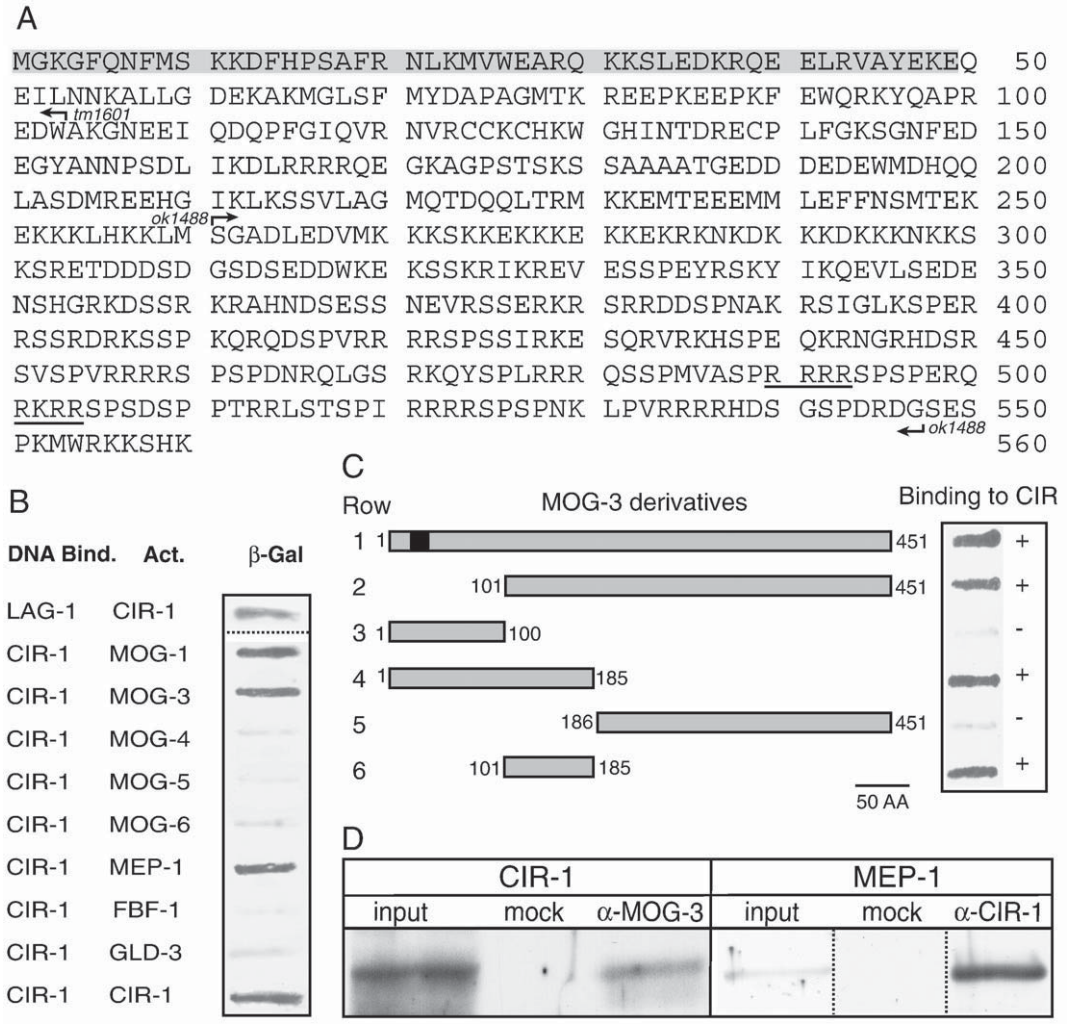

Fig. 4. CIR-1 binds to MOG-3. (A) Sequence of CIR-1. Predicted nuclear localization signals are underlined and the endpoints of deletion alleles *tm1601* and *ok1488* are indicated. Deletion *tm1601* starts 40 nt upstream of the coding region. The "N-terminal domain of CIR" which was used for the alignment in Fig. S3G is highlighted in gray. (B) Protein–protein interactions in the yeast two-hybrid system. Proteins were fused either to the LexA DNA binding domain or to the GAL4 activation domain as indicated. (C) The conserved motifs of MOG-3 are not necessary for CIR-1 binding. Boxes indicate MOG-3 derivatives. The minimal region of MOG-3 that is required for CIR-1 binding comprises residues 101 to 185. (row 6). (D) Protein extracts were immunoprecipitated with either anti-MOG-3 (left panel) or anti-CIR-1 (right panel) antibodies and analyzed by Western blotting using anti-CIR-1 (left panel) or anti-MEP-1 (right panel) antibodies. MEP-1 and CIR-1 migrated at 115 kD and 65 kD, respectively. Co-immunoprecipitations were performed with the corresponding preimmune sera in the mock controls. The input corresponds to 10% of protein extract used for immunoprecipitation.

Injection of double-stranded *cir-1* RNA, however, resulted in 100% of embryonic lethality among the progeny. Such embryos ceased development at late gastrulation (Fig. S3B). The phenotypes observed in *cir-1* deletion mutants and through *(cir-1)RNAi* indicate that *cir-1* is required maternally for embryonic development, while it is required zygotically for later development. To circumvent early larval phenotypes, we either fed gravid animals with bacteria producing double-stranded *cir-1* RNA or soaked L1 larvae in *cir-1* dsRNA (Tabara et al., 1998; Timmons and Fire, 1998). Typically, 30% to 40% of *cir-1(RNAi)*-treated animals developed a protruding vulva, indicating that *cir-1* is required for vulva formation (Figs. 6C,H). *cir-1(RNAi)* also affected germ line development in many aspects. Germ lines were often small and lacked mature germ cells (Fig. 6C). Others produced normal amounts of sperm (160 spermatids per gonadal arm). However, oogenesis was consistently defective in *cir-1(RNAi)*-treated N2 animals (Figs. 6C,D). To search for interactions between *cir-1* and genes involved in germ line development, we treated sex determination mutants with *cir-1(RNAi)*. Masculinized *mog-3* animals were not affected by *cir-1(RNAi)* at 25 °C (Fig. 6E). At permissive temperature, *cir-1(RNAi)*; *mog-3(q74)* animals were unaffected and produced both sperm and oocytes, like their control-incubated siblings (not shown). Feminized germ lines such as *fem-3(e1996)*, *gld-3(q730)* or *fog-1(q253ts)* have been examined (Barton and Kimble, 1990; Eckmann et al., 2002; Hodgkin, 1986). When treated with *cir-1(RNAi)*, *fem-3(e1996)* germ lines produced not only abnormally-shaped cells of various sizes, but also a few small oocyte-like cells known as ooïds (Fig. 6F). Nuclear morphology was observed by DAPI staining: germ nuclei apparently proceeded normally until pachytene, and some entered diplotene and diakinesis. However in most nuclei, chromosomes were not arranged as bivalents (Fig. 6F, insets). At 25 °C, the effect of *cir-1(RNAi)* on *fog-1(q253ts)* germ lines was less severe since less than 25% of the soaked L1 larvae developed germline defects similar to those observed in *fem-3* (data not shown). *gld-3(q730) cir-1(RNAi)* germ lines were partially defective since 50% of the treated larvae developed into adults that made no oocytes, 30% made few oocytes of abnormal shape, 10% were mainly tumorous, and the remaining 10% were unaffected (Figs. S3C–E). As expected, spermatogenesis was not observed in feminized mutants when subjected to *cir-1(RNAi)*.

Tumor formation can be a consequence of faulty *glp-1* signaling (Berry et al., 1997; Kadyk and Kimble, 1998). To search for a possible interaction between *cir-1* and *glp-1*, we knocked down *cir-1* in both

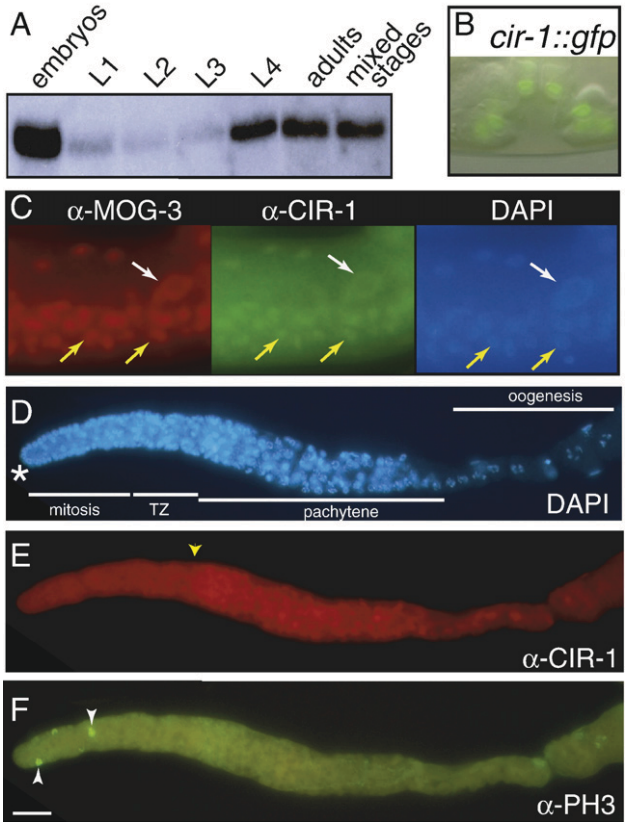

Fig. 5. Expression of *cir-1*. (A) Steady-state levels of the 1.7 kb *cir-1* mRNA vary during development in a manner similar to *mog-3* (Fig. 2A). (B) *cir-1::gfp* expression in the vulva. Nuclear CIR-1::GFP in the stacks of multinucleated toroidal cells that build up the L4 vulva. Merged DIC and epifluorescence images. (C) MOG-3 and CIR-1 are found in somatic and germ line nuclei. Magnification of a section of a late L4 larva stained with anti-MOG-3, anti-CIR-1 antibodies and DAPI. White and yellow arrows indicate intestinal and germ line nuclei, respectively. (D–F) Dissected wild type gonads stained with anti-CIR-1 and anti-PH3. CIR-1 is present in the meiotic region (E) and closely associated with DNA as shown by DAPI staining (D). The distal limit of CIR-1 expression is shown by a yellow arrowhead. Mitotic nuclei in the distal part of the germ line were stained by anti-PH3 antibodies (arrowheads, F). TZ, transition zone. The asterisk indicates the distal end. Scale bar, 10 μm.

glp-1 loss-of-function (lf) and gain-of-function (gf) mutants. *glp-1(lf)* animals were not affected by *cir-1(RNAi)*. In fact, *glp-1(lf);cir-1(RNAi)* germ lines were indistinguishable from *glp-1(lf)* germ lines that produce only a few spermatids (Austin and Kimble, 1987; not shown). In contrast, *glp-1(oz112gf)* mutants produce germ line tumors through accumulation of more than 4000 mitotic germ nuclei without showing any sign of meiosis (Berry et al., 1997). When treated with *cir-1(RNAi)*, *glp-1(gf)* mutants are still tumorous, but their germ lines contained significantly less germ cells: 1002 ± 107 nuclei versus more than 3000 nuclei in the control (Fig. 6H). In addition, germ line arm elongation was altered with an extra bend present in 5–10% of the animals observed (Red arrowheads in Fig. 6H). Taken together, we found that *cir-1* is essential for larval development and that it is necessary at later stages for robust germline proliferation, oogenesis and vulva formation. However in the absence of *gld-3*, *cir-1* is also necessary for progression of meiosis (Fig. S3C).

Discussion

MOG proteins are homologous to splicing factors

MOG proteins repress *fem-3* through its 3′ UTR (Gallegos et al., 1998). However, their action on *fem-3* might be indirect. Most MOG proteins are homologous to splicing factors (this work and Puoti and Kimble, 1999, 2000; Konishi et al., 2008). Therefore the most obvious possibility seems that defective or absent MOG proteins lead to altered splicing of *fem-3* or other mRNAs. Nevertheless, attempts to find abnormally spliced mRNAs failed (Belfiore et al., 2004; Puoti and Kimble, 1999; this study). Perhaps the splicing defects are subtle and difficult to detect? This possibility is supported by the finding that yeast Prp16 and Prp22 function in splicing fidelity (Mayas et al., 2006; Schwer, 2001). Therefore, one scenario is that in the absence of MOG proteins, weak splice sites might not be recognized and lead to alternatively spliced variants. Such abnormally spliced mRNAs could either be non functional, undergo degradation or code for dominant-negative gene products. On the other hand, MOG proteins could play an essential role in general splicing because in the absence of maternal *mog-1*, *mog-4* or *mog-5*, embryos die early during development (Graham and Kimble, 1993; Puoti and Kimble, 2000). Thus maternally-delivered wild type *mog* products could be sufficient to support somatic but not germ line development.

A nuclear complex containing MOG, CIR-1 and MEP-1

MEP-1 was identified as a binding partner of the DEAH-box proteins MOG-1, MOG-4 and MOG-5 (Belfiore et al., 2002). The presence of MOG-3 in the nucleus is provocative since regulators of the *fem-3* mRNA are expected to localize to the cytoplasm where they directly act on the 3′ UTR. Co-immunoprecipitations showed that MOG-3, MEP-1 and CIR-1 belong to a single complex. Furthermore the proteins appear to directly bind to each other in the yeast two-hybrid system. However we cannot exclude that additional proteins cooperate in this interaction. What is the significance of MOG-3 and CIR-1 binding? We speculate that this interaction might compensate for the N-terminal domain which is absent in nematode MOG-3. Furthermore, we hypothesize that the role of the nuclear complex on *fem-3* is indirect for the following reasons: First, neither MEP-1 nor the MOG proteins bind specifically to the regulatory element in the *fem-3* 3′ UTR (Belfiore et al., 2002 and unpublished results). Second, MOG, CIR-1 and MEP-1 do not bind to FBF. Third, while the loss-of-function phenotype of *mog* mutants is similar to a *fem-3* gain-of-function phenotype, *fem-3* is probably not the only target of *mog*. In fact, the maternal effect lethality phenotype that is associated to *mog* mutants has not been observed in *fbf* and *gld-3* animals. Furthermore, *fem-3(gf)* mutants produce far more sperm than *mog(lf)* mutants (Barton et al., 1987 and Figs. 1A,B). We therefore propose that the complex harboring MEP-1, CIR-1 and the MOG proteins controls the sperm–oocyte switch in a way that is distinct from FBF, GLD-3 and NOS-3. One possibility is that MEP-1, MOG-3 and CIR-1 function as epigenetical regulators. In fact, MEP-1 associates with LET-418, a member of the putative Nucleosome Remodelling and histone Deacetylase (NuRD) complex in *C. elegans* and mammalian CIR binds with histone deacetylase HDAC2, a component of the CSL co-repressor complex (Unhavaithaya et al., 2002; Hsieh et al., 1999). Histone deacetylation plays a crucial role in epigenetic control (de Moor et al., 2005; Lehrmann et al., 2002; Struhl, 1998). Therefore MOG-3 might control epigenetic modifications of genes that are directly or indirectly required for *fem-3* repression and meiosis progression. *fbf*, *mep-1* and *nos-3* are not likely to be such targets, since their mRNA levels are not significantly reduced in *mog-3* mutants. Nevertheless, subtle differences in protein expression might be sufficient to generate masculinized and/or tumorous germ lines. For example, the expansion of FBF expression throughout the pachytene region in *mog-3* hermaphrodites that have escaped sterility suggests that FBF is expressed ectopically in response to defective MOG-3 function at permissive temperature, perhaps to maintain oogenesis.

Another possibility comes from the finding that *Mut6p* codes for the MOG-1 homolog in *Chlamydomonas reinhardtii* and functions in transgene and transposon silencing (Wu-Scharf et al., 2000). Both

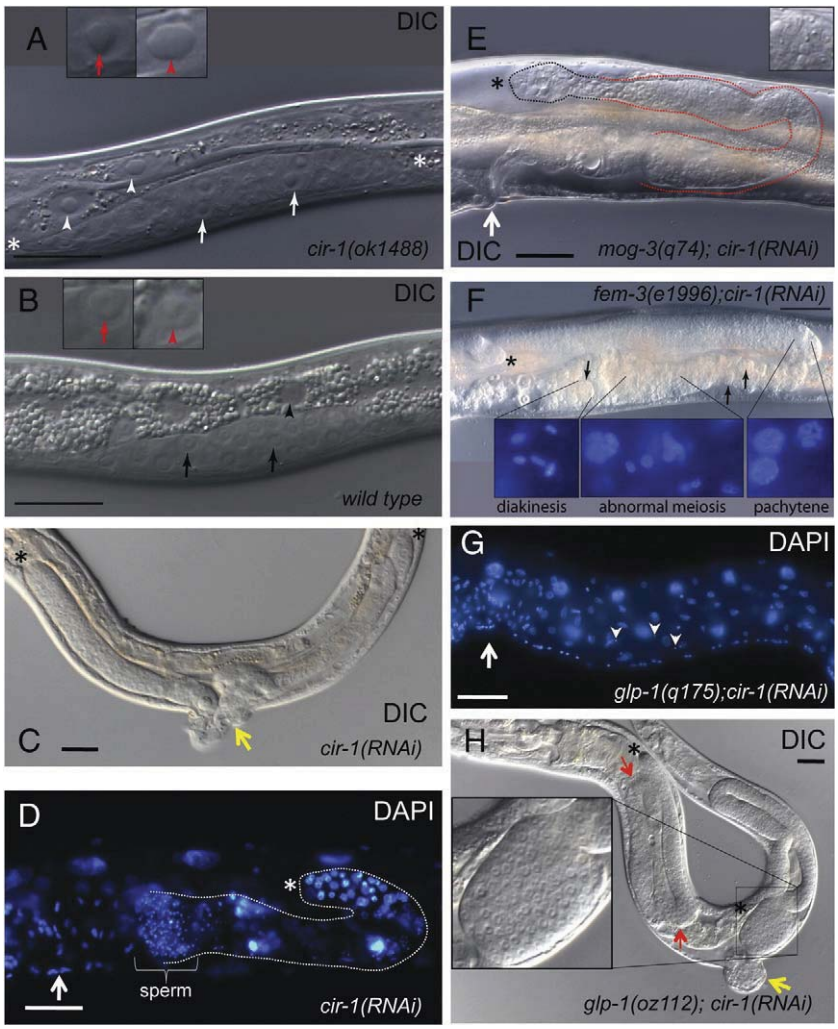

Fig. 6. The Cir-1 mutant phenotype. (A,B) *cir-1* is required for larval development. While most *cir-1(ok1488)* mutant larvae ceased development at L1, 10% arrested at L2 with abnormal nuclear morphology. Arrows point towards germline nuclei in mutant (white, A) and wild type L2 larvae (black, B). Arrowheads indicate somatic nuclei. Red arrows and red arrowheads point at germline and intestinal nucleoli, respectively. Nucleoli in *cir-1* L2 larvae are more refractive (see magnified insets). (C,D) Wild type L1 larvae soaked in double-stranded *cir-1* RNA developed into sterile adults with vulval defects (yellow arrows). Typically, *cir-1(RNAi)* germ lines are small, with either no mature germ cells (C) or normal amounts of sperm (D, one germ line arm is outlined). (E) RNA interference against *cir-1* did not alter germ line development in *mog-3* mutants at 25 °C. The germ line is comprised between the dotted curves; red dots indicate the region containing sperm. Sperm is shown in the magnified inset. (F) *fem-3(e1996) cir-1(RNAi)* females produce germ nuclei that enter meiotic pachytene and a few ooïds in the distal portion of the germ line (arrows). Nuclear morphology of ooïds as observed by DAPI staining under high magnification (F, insets): pachytene chromosomes appear as threads; nuclei in diakinesis normally contain six segregating bivalents. Such bivalents are absent in most nuclei in the distal portion of a *cir-1(RNAi)*-treated germ line. Towards the proximal end of the germ line, chromosomes form disorganized clusters, indicating defective progression of meiosis. (G) The germ line in *glp-1* loss-of-function mutants was not affected by *cir-1(RNAi)* and made 8 to 16 spermatids (white arrowheads). (H) *glp-1(oz112)* gain-of-function mutants are tumorous upon *cir-1(RNAi)* treatment (inset shows mitotic germ cells at the proximal end of the germ line). White arrows point towards a normal vulva. Asterisks indicate the distal end of the germ line. DIC: differential interference contrast (Nomarski). Bar, 10 µm.

mechanisms use small RNAs that interfere with gene expression by targeting either chromatin or other RNAs (Meister and Tuschl, 2004; Mello and Conte, 2004). Therefore *mog* and perhaps *cir-1* and *mep-1* might function in the production or the activity of small RNAs.

Finally, as mentioned above, the nuclear complex containing MEP-1, MOG-3 and CIR-1 could play a role in pre-mRNA splicing. This possibility is supported by the finding that in addition to its role as a transcriptional co-repressor, mammalian CIR modifies the splicing pattern of a reporter minigene in HeLa cells (Maita et al., 2005).

A role of MOG-3 and CIR-1 in meiosis

In addition to promoting the switch from spermatogenesis to oogenesis, *mog-3* is necessary for meiosis. Other sex determining genes also function in meiosis (Crittenden et al., 2002; Kraemer et al., 1999; Kadyk and Kimble, 1998; Eckmann et al., 2004; Thompson et al., 2005; Belfiore et al., 2004). In *C. elegans* hermaphrodites, meiosis is directed by two redundant pathways that function downstream of Notch (Hansen et al., 2004b). We now show that *mog-3* functions synergistically with *gld-3* or *gld-2* to promote meiosis progression. Such synergy is weak between *mog-3* and *gld-1* and was not observed between *mog-3* and *nos-3*. Therefore, *mog-3* functions either in the same branch as *gld-1* or in an alternative pathway (M. Hanazawa and T. Schedl, personal communication).

glp-1 represses *gld-1*, *gld-2* and *gld-3* to promote germ line proliferation to the detriment of meiosis (Berry et al., 1997; Eckmann et al., 2004; Kadyk and Kimble, 1998). Ligands of GLP-1/Notch trigger the cleavage of the intracellular domain of the GLP-1 receptor, which translocates to the nucleus where it removes CSL repressors and recruits transcriptional activators (for review see Greenwald, 2005). CIR was first identified as a transcriptional co-repressor of CBF1 which directly binds to CSL (Hsieh et al., 1999). Similarly to its mammalian ortholog, CIR-1 binds not only to the CSL protein LAG-1 but also to MOG-3. Like *lag-1* mutants, most *cir-1* mutants arrest development at

the L1 stage. However, typical features of arrested *lag-1* larvae were not observed with *cir-1* (Lambie and Kimble, 1991). Adult *cir-1(RNAi)* germ lines are generally small and underproliferative. These occasionally produce sperm, but are often defective in oogenesis. *mog-3* animals were unaffected by *cir-1(RNAi)*, indicating that *cir-1* is not necessary for spermatogenesis. However, this result should also be considered in the light of spermatogenesis being less sensitive to RNAi than oogenesis (Kim et al., 2005; Reinke et al., 2004). Feminized germ lines treated with *cir-1(RNAi)* showed phenotypes of different strengths. While oocyte production was impaired in *fem-3(lf)* and *fog-1* mutants, we observed tumorous germ lines in a *gld-3* mutant background. Therefore like *mog-3*, *cir-1* functions synthetically with *gld-3* in meiosis progression. How can a role of *cir-1* in meiosis be reconciled with its requirement for robust germ line proliferation? One explanation is that the various Cir-1 phenotypes depend on different levels of gene inactivation by RNA interference. Therefore *cir-1* is necessary for different aspects of germ line development, from proliferation and gonad arm extension, to progression of meiosis. The presence of CIR-1 in the meiotic region of the germ line at least supports its role in meiosis. Finally, *cir-1* could also function in the soma and promote germ cell proliferation and sex determination by signaling from somatic sheath or spermathecal cells (McCarter et al., 1997).

Acknowledgments

We are grateful to Judith Kimble and Tim Schedl for *mog-3* mutants. Thanks go to Pamela Bianchi for sharing results. Some nematode strains used in this work were provided by the CGC, which is funded by the NIH. Other strains were from the National Bio Resource Project in Japan. A.P. was supported by the Swiss National Science Foundation (Grant 3100-67052).

Appendix A. Supplementary data

Supplementary data associated with this article can be found, in the online version, at doi:10.1016/j.ydbio.2010.05.009.

References

Ahringer, J., Kimble, J., 1991. Control of the sperm–oocyte switch in *Caenorhabditis elegans* hermaphrodites by the *fem-3* 3′ untranslated region. Nature 349, 346–348.
Ahringer, J., Rosenquist, T.A., Lawson, D.N., Kimble, J., 1992. The *Caenorhabditis elegans* sex determining gene *fem-3* is regulated post-transcriptionally. EMBO J. 11, 2303–2310.
Austin, J., Kimble, J., 1987. *glp-1* is required in the germ line for regulation of the decision between mitosis and meiosis in *C. elegans*. Cell 51, 589–599.
Bai, C., Elledge, S.J., 1997. Searching for interacting proteins with the two-hybrid system I. Oxford University Press, Oxford, UK.
Bartel, P.L., Fields, S., 1995. Analyzing protein–protein interactions using two-hybrid system. Meth. Enzymol. 254, 241–263.
Barton, M.K., Kimble, J., 1990. *fog-1*, a regulatory gene required for specification of spermatogenesis in the germ line of *Caenorhabditis elegans*. Genetics 125, 29–39.
Barton, M.K., Schedl, T.B., Kimble, J., 1987. Gain-of-function mutations of *fem-3*, a sex-determination gene in *Caenorhabditis elegans*. Genetics 115, 107–119.
Belfiore, M., Mathies, L.D., Pugnale, P., Moulder, G., Barstead, R., Kimble, J., Puoti, A., 2002. The MEP-1 zinc-finger protein acts with MOG DEAH box proteins to control gene expression via the *fem-3* 3′ untranslated region in *Caenorhabditis elegans*. RNA 8, 725–739.
Belfiore, M., Pugnale, P., Saudan, Z., Puoti, A., 2004. Roles of the *C. elegans* cyclophilin-like protein MOG-6 in MEP-1 binding and germline fates. Development 131, 2935–2945.
Berry, L.W., Westlund, B., Schedl, T., 1997. Germ-line tumor formation caused by activation of *glp-1*, a *Caenorhabditis elegans* member of the Notch family of receptors. Development 124, 925–936.
Bettinger, J.C., Lee, K., Rougvie, A.E., 1996. Stage-specific accumulation of the terminal differentiation factor LIN-29 during *Caenorhabditis elegans* development. Development 122, 2517–2527.
Brenner, S., 1974. The genetics of *Caenorhabditis elegans*. Genetics 77, 71–94.
Chiu, Y.F., Liu, Y.C., Chiang, T.W., Yeh, T.C., Tseng, C.K., Wu, N.Y., Cheng, S.C., 2009. Cwc25 is a novel splicing factor required after Prp2 and Yju2 to facilitate the first catalytic reaction. Mol. Cell. Biol. 29, 5671–5678.
Crittenden, S.L., Bernstein, D.S., Bachorik, J.L., Thompson, B.E., Gallegos, M., Petcherski, A.G., Moulder, G., Barstead, R., Wickens, M., Kimble, J., 2002. A conserved RNA-binding protein controls germline stem cells in *Caenorhabditis elegans*. Nature 417, 660–663.
de Moor, C.H., Meijer, H., Lissenden, S., 2005. Mechanisms of translational control by the 3′ UTR in development and differentiation. Semin. Cell Dev. Biol. 16, 49–58.
Eckmann, C.R., Kraemer, B., Wickens, M., Kimble, J., 2002. GLD-3, a bicaudal-C homolog that inhibits FBF to control germline sex determination in *C. elegans*. Dev. Cell 3, 697–710.
Eckmann, C.R., Crittenden, S.L., Suh, N., Kimble, J., 2004. GLD-3 and control of the mitosis/meiosis decision in the germline of *Caenorhabditis elegans*. Genetics 168, 147–160.
Francis, R., Barton, M.K., Kimble, J., Schedl, T., 1995. *gld-1*, a tumor suppressor gene required for oocyte development in *Caenorhabditis elegans*. Genetics 139, 579–606.
Fu, X.D., 1995. The superfamily of arginine/serine-rich splicing factors. RNA 1, 663–680.
Gallegos, M., Ahringer, J., Crittenden, S., Kimble, J., 1998. Repression by the 3′ UTR of *fem-3*, a sex-determining gene, relies on a ubiquitous *mog*-dependent control in *Caenorhabditis elegans*. EMBO J. 17, 6337–6347.
Graham, P.L., Kimble, J., 1993. The *mog-1* gene is required for the switch from spermatogenesis to oogenesis in *Caenorhabditis elegans*. Genetics 133, 919–931.
Graham, P.L., Schedl, T., Kimble, J., 1993. More *mog* genes that influence the switch from spermatogenesis to oogenesis in the hermaphrodite germ line of *Caenorhabditis elegans*. Dev. Genet. 14, 471–484.
Greenwald, I., 2005. LIN-12/Notch signaling in *C. elegans*. WormBook, ed. The *C. elegans* Research Community, WormBook, doi:10.1895/wormbook.1.10.1, http://www.wormbook.org.
Hansen, D., Hubbard, E.J., Schedl, T., 2004a. Multi-pathway control of the proliferation versus meiotic development decision in the *Caenorhabditis elegans* germline. Dev. Biol. 268, 342–357.
Hansen, D., Wilson-Berry, L., Dang, T., Schedl, T., 2004b. Control of the proliferation versus meiotic development decision in the *C. elegans* germline through regulation of GLD-1 protein accumulation. Development 131, 93–104.
Hodgkin, J., 1986. Sex determination in the nematode *C. elegans*: analysis of *tra-3* suppressors and characterization of *fem* genes. Genetics 114, 15–52.
Hsieh, J.J., Zhou, S., Chen, L., Young, D.B., Hayward, S.D., 1999. CIR, a corepressor linking the DNA binding factor CBF1 to the histone deacetylase complex. Proc. Natl. Acad. Sci. U. S. A. 96, 23–28.
Hubbard, E.J., Greenstein, D., 2005. Introduction to the germ line. WormBook 1–4.
Jakubowski, J., Kornfeld, K., 1999. A local, high-density, single-nucleotide polymorphism map used to clone *Caenorhabditis elegans cdf-1*. Genetics 153, 743–752.
Kadyk, L.C., Kimble, J., 1998. Genetic regulation of entry into meiosis in *Caenorhabditis elegans*. Development 125, 1803–1813.
Kim, J.K., Gabel, H.W., Kamath, R.S., Tewari, M., Pasquinelli, A., Rual, J.F., Kennedy, S., Dybbs, M., Bertin, N., Kaplan, J.M., Vidal, M., Ruvkun, G., 2005. Functional genomic analysis of RNA interference in *C. elegans*. Science 308, 1164–1167.
Kim, W.K., Nykamp, K., Suh, N., Bachorik, J.L., Wang, L., Kimble, J., 2009. Antagonism between GLD-2 binding partners controls gamete sex. Dev. Cell 16, 723–733.
Kimble, J., Crittenden, S.L., 2007. Controls of germline stem cells, entry into meiosis, and the sperm/oocyte decision in *Caenorhabditis elegans*. Annu. Rev. Cell Dev. Biol. 23, 405–433.
Konishi, T., Uodome, N., Sugimoto, A., 2008. The *Caenorhabditis elegans* DDX-23, a homolog of yeast splicing factor PRP28, is required for the sperm–oocyte switch and differentiation of various cell types. Dev. Dyn. 237, 2367–2377.
Kraemer, B., Crittenden, S., Gallegos, M., Moulder, G., Barstead, R., Kimble, J., Wickens, M., 1999. NANOS-3 and FBF proteins physically interact to control the sperm–oocyte switch in *Caenorhabditis elegans*. Curr. Biol. 9, 1009–1018.
Lambie, E.J., Kimble, J., 1991. Two homologous regulatory genes, *lin-12* and *glp-1*, have overlapping functions. Development 112, 231–240.
Lamont, L.B., Crittenden, S.L., Bernstein, D., Wickens, M., Kimble, J., 2004. FBF-1 and FBF-2 regulate the size of the mitotic region in the *C. elegans* germline. Dev. Cell 7, 697–707.
Lehrmann, H., Pritchard, L.L., Harel-Bellan, A., 2002. Histone acetyltransferases and deacetylases in the control of cell proliferation and differentiation. Adv. Cancer Res. 86, 41–65.
Maita, H., Kitaura, H., Ariga, H., Iguchi-Ariga, S.M.M., 2005. CIR, a co-repressor of CBF1, binds to PAP-1 and effects alternative splicing. Exp. Cell Res. 303, 375–387.
Marchler-Bauer, A., Anderson, J.B., Chitsaz, F., Derbyshire, M.K., DeWeese-Scott, C., Fong, J.H., Geer, L.Y., Geer, R.C., Gonzales, N.R., Gwadz, M., He, S., Hurwitz, D.I., Jackson, J.D., Ke, Z., Lanczycki, C.J., Liebert, C.A., Liu, C., Lu, F., Lu, S., Marchler, G.H., Mullokandov, M., Song, J.S., Tasneem, A., Thanki, N., Yamashita, R.A., Zhang, D., Zhang, N., Bryant, S.H., 2009. CDD: specific functional annotation with the Conserved Domain Database. Nucleic Acids Res. 37, D205–210.
Mayas, R.M., Maita, H., Staley, J.P., 2006. Exon ligation is proofread by the DExD/H-box ATPase Prp22p. Nat. Struct. Mol. Biol. 13, 482–490.
McCarter, J., Bartlett, B., Dang, T., Schedl, T., 1997. Soma–germ cell interactions in *Caenorhabditis elegans*: multiple events of hermaphrodite germline development require the somatic sheath and spermathecal lineages. Dev. Biol. 181, 121–143.
Meister, G., Tuschl, T., 2004. Mechanisms of gene silencing by double-stranded RNA. Nature 431, 343–349.
Mello, C.C., Conte Jr., D., 2004. Revealing the world of RNA interference. Nature 431, 338–342.
Ohi, M.D., Link, A.J., Ren, L., Jennings, J.L., McDonald, W.H., Gould, K.L., 2002. Proteomics analysis reveals stable multiprotein complexes in both fission and budding yeasts containing Myb-related Cdc5p/Cef1p, novel pre-mRNA splicing factors, and snRNAs. Mol. Cell. Biol. 22, 2011–2024.
Puoti, A., Kimble, J., 1999. The *Caenorhabditis elegans* sex determination gene *mog-1* encodes a member of the DEAH-Box protein family. Mol. Cell. Biol. 19, 2189–2197.
Puoti, A., Kimble, J., 2000. The hermaphrodite sperm/oocyte switch requires the *Caenorhabditis elegans* homologs of PRP2 and PRP22. Proc. Natl. Acad. Sci. U. S. A. 97, 3276–3281.

Reinke, V., Gil, I.S., Ward, S., Kazmer, K., 2004. Genome-wide germline-enriched and sex-biased expression profiles in *Caenorhabditis elegans*. Development 131, 311–323.
Schwer, B., 2001. A new twist on RNA helicases: DExH/D box proteins as RNPases. Nat. Struct. Biol. 8, 113–116.
Struhl, K., 1998. Histone acetylation and transcriptional regulatory mechanisms. Genes Dev. 12, 599–606.
Subramaniam, K., Seydoux, G., 1999. *nos-1* and *nos-2*, two genes related to *Drosophila nanos*, regulate primordial germ cell development and survival in *Caenorhabditis elegans*. Development 126, 4861–4871.
Tabara, H., Grishok, A., Mello, C.C., 1998. RNAi in *C. elegans*: soaking in the genome sequence. Science 282, 430–431.
Thompson, B.E., Bernstein, D.S., Bachorik, J.L., Petcherski, A.G., Wickens, M., Kimble, J., 2005. Dose-dependent control of proliferation and sperm specification by FOG-1/CPEB. Development 132, 3471–3481.
Timmons, L., Fire, A., 1998. Specific interference by ingested dsRNA. Nature 395, 854.
Unhavaithaya, Y., Shin, T.H., Miliaras, N., Lee, J., Oyama, T., Mello, C.C., 2002. MEP-1 and a homolog of the NURD complex component Mi-2 act together to maintain germline–soma distinctions in *C. elegans*. Cell 111, 991–1002.
Wu-Scharf, D., Jeong, B., Zhang, C., Cerutti, H., 2000. Transgene and transposon silencing in *Chlamydomonas reinhardtii* by a DEAH-box RNA helicase. Science 290, 1159–1162.
Zhang, B., Gallegos, M., Puoti, A., Durkin, E., Fields, S., Kimble, J., Wickens, M.P., 1997. A conserved RNA-binding protein that regulates sexual fates in the *C. elegans* hermaphrodite germ line. Nature 390, 477–484.